Biosensor Based on Ultrasmall MoS₂ Nanoparticles for Electrochemical Detection of H₂O₂ Released by Cells at the Nanomolar Level

Tanyuan Wang,[†] Haichuan Zhu,[‡] Junqiao Zhuo,[†] Zhiwei Zhu,[†] Pagona Papakonstantinou,[§] Gennady Lubarsky,[§] Jian Lin,*[‡] and Meixian Li*[†]

[†]Institute of Analytical Chemistry, College of Chemistry and Molecular Engineering, Peking University, Beijing 100871, P. R. China
[‡]Synthetic and Functional Biomolecules Center, College of Chemistry and Molecular Engineering, Peking University, Beijing 100871, P. R. China
[§]School of Engineering, Engineering Research Institute, University of Ulster, Newtownabbey BT37 0QB, U.K.

Ⓢ Supporting Information

ABSTRACT: Monodispersed surfactant-free MoS₂ nanoparticles with sizes of less than 2 nm were prepared from bulk MoS₂ by simple ultrasonication and gradient centrifugation. The ultrasmall MoS₂ nanoparticles expose a large fraction of edge sites, along with their high surface area, which lead to attractive electrocatalytic activity for reduction of H₂O₂. An extremely sensitive H₂O₂ biosensor based on MoS₂ nanoparticles with a real determination limit as low as 2.5 nM and wide linear range of 5 orders of magnitude was constructed. On the basis of this biosensor, the trace amount of H₂O₂ released from Raw 264.7 cells was successfully recorded, and an efficient glucose biosensor was also fabricated. Since H₂O₂ is a byproduct of many oxidative biological reactions, this work serves as a pathway for the application of MoS₂ in the fields of electrochemical sensing and bioanalysis.
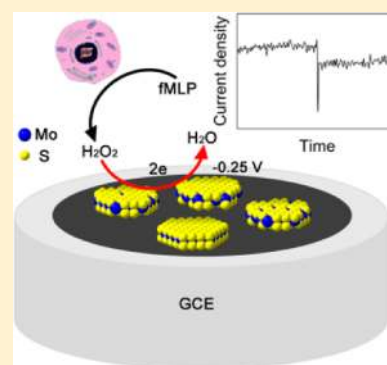
The rapid and accurate detection of hydrogen peroxide (H₂O₂) is of practical importance in the fields of bioanalysis as well as food security and environmental protection.[1,2] H₂O₂, a product of incomplete reduction of O₂, is generated as a byproduct of a wide range of biological processes.[3,4] It is also suggested to be involved in the function and signal transduction of the cells.[5−7] Therefore, highly sensitive determination of H₂O₂ is necessary and vital, and various H₂O₂ detection and measurement methods have been explored, including fluorometry,[8] spectrophotometry,[9] cell imaging,[10,11] electrochemical methods,[12−22] and so on. Among them, the electrochemical techniques have attracted much more attention due to their great advantages include high sensitivity and selectivity, rapid response, low cost, simple instrumentation, easy miniaturization and good quantitative ability. Especially, nanomaterials including precious metal nanoparticles,[23,24] carbon nanomaterials,[25,26] and metallic oxide nanostructures,[27,28] etc. play key roles in construction of H₂O₂ electrochemical sensors due to their unique electronic and catalytic properties as well as their good stability. The resulting electrochemical biosensors showed highly electrocatalytic activity toward the reduction or oxidization of H₂O₂. However, so far most of the reported H₂O₂ electrochemical sensors could only reach a detection limit of sub-micromolar level,[12,29,30] which are inadequate for monitoring nanomolar level of H₂O₂ produced in cellular activities; whereas, those which were capable of measuring H₂O₂ with extremely high sensitivity usually used horseradish peroxidase (HRP), mediators, or precious metal nanoparticles[31−34] which would result in the problems of the low long-term operational stability and rising cost. Herein, we demonstrate that ultrasmall MoS₂ nanoparticles obtained by a very simple process can act as an excellent catalyst. It shows highly electrocatalytic activity toward reduction of H₂O₂ and achieves highly sensitive detection of H₂O₂ at the nanomolar level.

MoS₂ is a kind of layered materials that is commercially used as a solid lubricant and also a catalyst for hydrodesulfurization reaction.[35] Recent study also proves that it could be as a promising candidate for the catalyst of the hydrogen evolution reaction (HER).[36−39] Since it shows similar structure to graphene, it attracts great attention in the fields of nano-electronics and optoelectronics.[40,41] Although MoS₂ is expected to be employed for the construction of the biosensors like graphene,[42−45] so far little research has been done in this respect. Its electrocatalytical performance is also rarely studied except for hydrodesulfurization reaction and hydrogen evolution reaction.[46,47] On the basis of our previous work on its electrocatalytical activity for oxygen reduction reaction (ORR),[48] in this work, we discover the electrocatalytical activity

of MoS$_2$ nanoparticles toward the reduction of H$_2$O$_2$ and construct an extremely sensitive H$_2$O$_2$ biosensor based on it. We also demonstrate that this biosensor could successfully detect the trace amount of H$_2$O$_2$ released by cells. In addition, this H$_2$O$_2$ biosensor could be applicable to the indirect measurement of the other biomolecules through the detection of hydrogen peroxide like glucose since H$_2$O$_2$ is a product of many oxidative biological reactions.[49−52]

■ EXPERIMENTAL SECTION

Preparation of MoS$_2$ Nanoparticles. MoS$_2$ (99%, 2 μm in size, Aldrich) was mixed with DMF (99.9%, Aldrich) at a concentration of 1 mg mL^{-1}. This mixture was ultrasonicated by a SB-2200 sonifier (Shanghai Branson, China) at room temperature (22 ± 2 °C) for 4 h to form a black suspension. After that the suspension was centrifuged at 1000 rpm for 15 min, 3000 rpm for 15 min and 6000 rpm for 30 min successively. The precipitates were collected, respectively, for the control experiments. Then the supernatant was centrifuged at 12 000 rpm for 30 min and the precipitation was gathered. A GS-15R centrifugation system (Beckman, America) was used for these procedures.

Fabrication of H$_2$O$_2$ Biosensors and Glucose Biosensors Based on MoS$_2$ Nanoparticles. MoS$_2$ nanoparticles were dispersed into DMF with a concentration of approximate 1 mg mL^{-1}. Then the solutions were dropped on the GC electrodes (diameter = 3 mm or 5 mm) and dried in the air with a loading of 0.2 mg cm^{-2}. The MoS$_2$ nanoparticles would form very stable films even without the protection of Nafion. This modified electrode was then washed with deionized water five times to avoid the possible influence of the residual DMF for the following experiments. For the glucose biosensor, 5 mg mL^{-1} glucose oxidase (TOYOBO) was immobilized on the MoS$_2$ nanoparticle film by the simple drop-casting method with a loading of 0.2 mg cm^{-2}, and then 3 μL of 0.05% Nafion (Aldrich) was dropped on the modified electrode to form a protective layer.

Detection of H$_2$O$_2$ Released from RAW 264.7 Cells. Raw 264.7 cells (obtained from Peking Union Medical College) were grown in 5% CO$_2$ in 75 cm^2 flasks containing Dulbecco's modified Eagle's medium with 1% antibiotics and 10% (v/v) fetal bovine serum (FBS) at 37 °C. After growing to 90% confluence, the cells were collected by centrifugation and washed with PBS three times. The number of the cells was counted by a hemocytometer. During the test, a pellet that contained 2 × 10^6 cells was resuspended into 20 mL of PBS (0.1 M, pH = 7.4) and the mixture was saturated with N$_2$. As a control group, 20 μL of catalase (340 000−1 360 000 units mL^{-1}, Aldrich) was added to the solution that contained cells. A potential of −0.25 V (vs SCE) was applied to the MoS$_2$ nanoparticle modified electrode. A 0.3 μM solution of N-formylmethionyl-leucyl-phenylalanine (fMLP, 97%, Aldrich) was added into the solution after a steady background noise was obtained.

Characterization. All electrochemical measurements were carried out on a CHI 660D (Chenhua, China) at room temperature. A Pt electrode was used as the counter electrode and a GC or MoS$_2$ modified GC electrode was used as the working electrode. A saturated calomel electrode (SCE) was used as the reference electrode for all the electrochemical tests. The rotation speed of the electrode was controlled by a modulated speed rotator (Pine, America). All the solutions were saturated with N$_2$ during the measurement of H$_2$O$_2$. A

transmission electron microscopy (TEM) image was acquired on a JEM-2100F electron microscope (JEOL, Japan). Scanning electron microscopy (SEM) images were obtained on a S-4800 electron microscope (Hitach, Japan). An atomic force microscopy (AFM) image was carried out on Nanoscope III a AFM (Veeco, America). X-ray photoelectron spectra (XPS) were collected on an Axis Ultra spectrometer (Kratos Analytical Ltd., Japan) and the binding energy was calibrated by the C 1s peak at 284.8 eV.

■ RESULTS AND DISCUSSION

Ultrasonication was proved to be an easy and efficient way to exfoliate graphite, bulk MoS$_2$, and some other layered materials into a single layer.[53−56] However, our previous research revealed that in addition to single layered MoS$_2$, ultrasmall MoS$_2$ nanoparticles with large amounts of surface defects were also present in the exfoliation process.[57] By a combination of ultrasonication and gradient centrifugation, MoS$_2$ nanoparticles with a narrow size distribution could be obtained. Figure 1a was
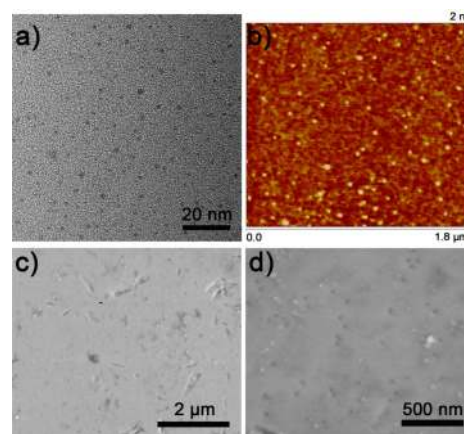

Figure 1. (a) TEM image of the MoS$_2$ nanoparticles, (b) AFM image of the MoS$_2$ nanoparticles, (c) SEM image of the MoS$_2$ nanoparticles modified film, and (d) SEM image of the MoS$_2$ nanoparticles modified film with higher resolution.

the transmission electron microscopy (TEM) image of the prepared MoS$_2$ nanoparticles. These particles showed a diameter of about 1−2 nm. The average size of the nanoparticles was 1.47 ± 0.16 nm, and most of the particles were amorphous, as was revealed in our earlier work.[57] Atomic force microscopic (AFM) characterization further confirmed that these as-prepared MoS$_2$ nanoparticles were monodispersed (Figure 1b). The height of these nanoparticles ranged from 1 to 2.5 nm (Figure S1 in the Supporting Information), which matched well with the particle size observed from the TEM image. MoS$_2$ nanoparticle dispersion casted on the surface of a glassy carbon (GC) electrode led to the formation of a relatively compact film. As shown in Figure 1c,d, only several particles with sizes of tens of nanometers could be observed on the surface of the modified GC electrode in addition to the hollows. These relatively larger particles originated from the unavoidable self-agglomeration of the ultrasmall MoS$_2$ particles since no surfactant was used for the protection of the nanoparticles. X-ray photoelectron spectroscopy (XPS) was also used for the elemental composition and bonding configuration characterization of the modified electrodes. Typical Mo 3d peaks and S 2p peaks could be observed

(Figures S2 and S3 in the Supporting Information), and the ratio of Mo to S was calculated to be 1:2.1, which verified that the average composition of the as-prepared nanoparticles was MoS_2.

We evaluated the electrocatalytic activity of the MoS_2 nanoparticle modified GC electrode toward reduction of H_2O_2 in 0.1 M PBS (pH = 7.4) with the protection of N_2. Figure 2 showed the cyclic voltammetric (CV) responses of the
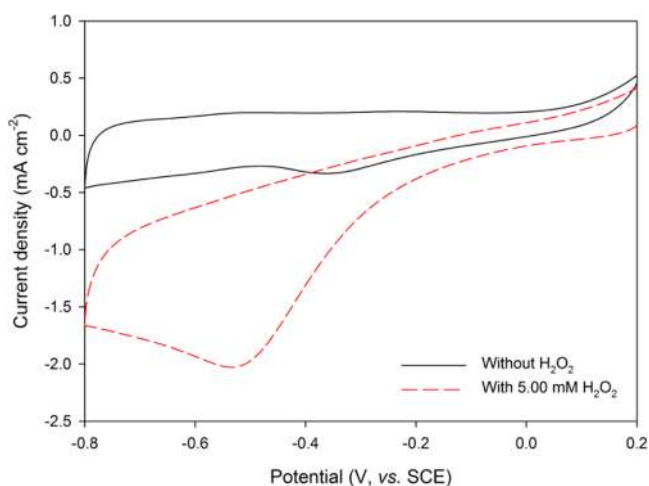

Figure 2. CV of the ultrasmall MoS_2 nanoparticles modified electrode with and without 5.00 mM H_2O_2 in the N_2 saturated 0.1 M PBS at a scan rate of 50 mV s^{-1}.

ultrasmall MoS_2 nanoparticles in the absence and presence of 5.00 mM H_2O_2. A small reduction peak at about −0.4 V was observed in the absence of H_2O_2, which might originate from their surface defects. However, after the addition of H_2O_2, the reduction current increased greatly, which was quite different from the bare GC electrode (Figure S4 in the Supporting Information). Bulk MoS_2, MoS_2 layer, and larger MoS_2 nanoparticles with sizes of tens of nanometers collected at lower centrifugation speeds by the ultrasonication-centrifugation method as reported in our previous work[48] were also used to modify the GC electrodes, respectively, and their electrocatalytical activities toward the reduction of H_2O_2 were studied and compared with that of the smallest MoS_2 nanoparticles (1−2 nm, collected at 12 000 rpm). Figures S5−S8 in the Supporting Information displayed their CV responses. Comparison of current density measurements (per geometric area) at negative potentials revealed a clear trend that the current responses increased with a decrease of the MoS_2 particle sizes. These suggested that the catalytic activity of the MoS_2 nanoparticles was associated with its surface active sites and effective surface areas of the electrodes. The ultrasmall MoS_2 nanoparticles collected at the highest centrifugal speed exhibited the maximum amounts of unsaturated catalytically active edge sites as well as the largest surface to volume ratios,[57] resulting in the best electrocatalytical performance toward the reduction of H_2O_2.

This excellent catalytic activity was used to construct the biosensor for detection of H_2O_2 using chronoamperometry. Figure 3a,b showed the typical current−time (i−t) curves of the ultrasmall MoS_2 nanoparticle modified GC electrode with the successive addition of H_2O_2 into the stirred N_2 saturated 0.1 M PBS at −0.25 V. Even though more negative applied potentials would lead to a larger current response, an applied potential of
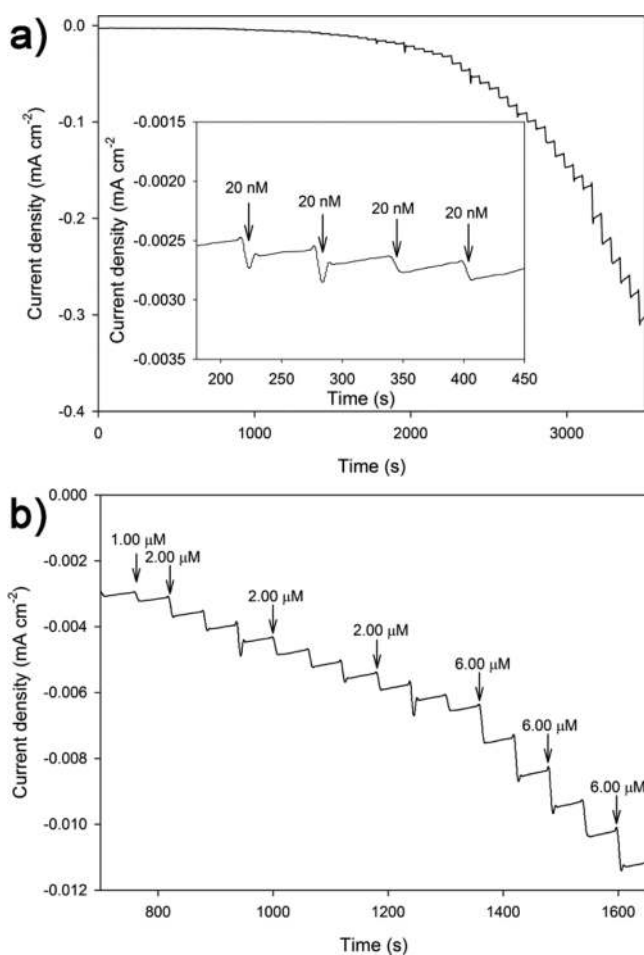

Figure 3. (a) Amperometric responses of the ultrasmall MoS_2 nanoparticles modified electrode to the successive addition of H_2O_2 in the N_2 saturated 0.1 M PBS at −0.25 V. The inset shows a close look of the response current to 20 nM H_2O_2. (b) A close look of the response current of the ultrasmall MoS_2 nanoparticles modified electrode to several micromolar H_2O_2.

−0.25 V was selected in order to avoid the possible interference of O_2 reduction. Under this potential, no current response could be observed with the injection of deionized water (Figure S9 in the Supporting Information), which suggested that O_2 reduction had no effect on H_2O_2 detection. After the addition of H_2O_2, this sensor could achieve the steady-state current within 5 s, which indicated fast response time. Besides, obvious current response could be observed with the addition of H_2O_2 from several nanomolar to tens of millimolar for the sensor (Figure 4), which suggested that this MoS_2-based sensor could be applied to a great many systems that contain H_2O_2 with different concentrations.

What is amazing was that the sensor was extremely sensitive to H_2O_2 concentration at a level of nanomolar. It demonstrated a wide linear range over the concentration of H_2O_2 from 5.0 nM to 100 nM with a sensitivity as high as 2.58×10^3 mA cm^{-2} M^{-1} (Figure 5a) and from 100 nM to 100 μM with a detection sensitivity of 160 mA cm^{-2} M^{-1} (Figure 5b). The possible reason for its higher sensitivity at lower H_2O_2 concentration was that the H_2O_2 molecules freely diffused and reached the films at very low concentrations, and there was no interaction between molecules, leading to high sensitivity. In contrast, the H_2O_2 molecular interaction at high concentrations resulted in
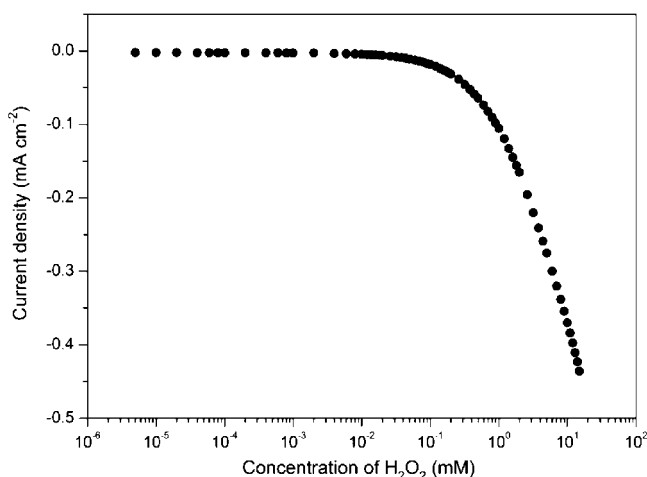
Figure 4. Current response of the electrode to logarithm of the H_2O_2 concentration.
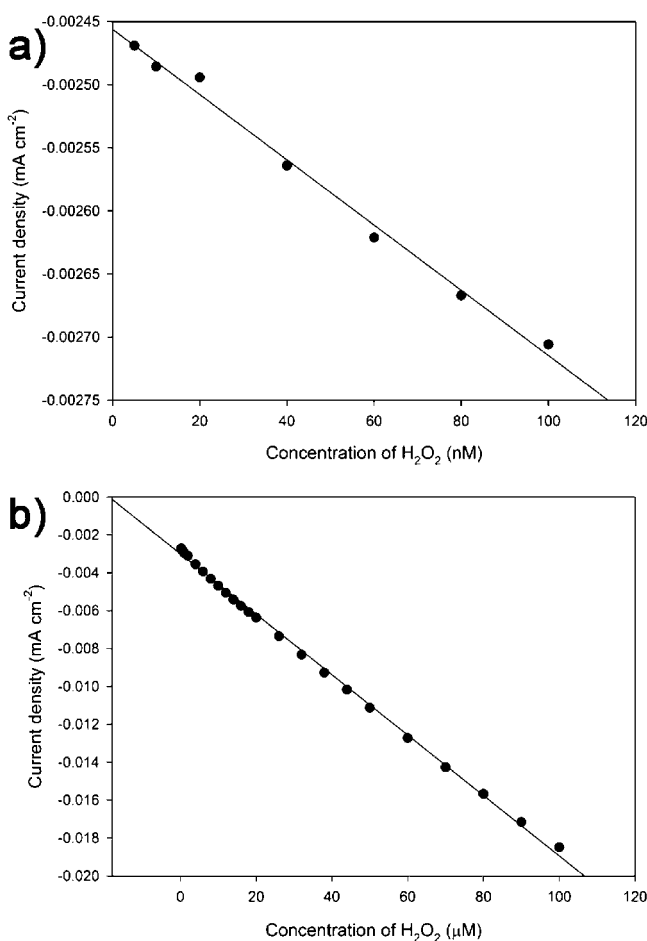

Figure 5. (a) Calibration curve of the amperometric response to the concentration of H_2O_2 from 5.0 nM to 100 nM. (b) Calibration curve of the amperometric response to the concentration of H_2O_2 from 0.100 μM to 100 μM.

low sensitivity, as reported in the literature.[58] Besides, the large proportion of surface defects and high surface-to-volume ratio of these ultrasmall nanoparticles might also contribute to it.

In order to further verify the size dependence of MoS_2 sensitivity to the detection of H_2O_2, the amperometric responses of different electrodes modified with the MoS_2

particles collected at lower centrifugation speeds as well as that of the bare GC electrode were also investigated for the reduction of H_2O_2 (Figures S10−S14 in the Supporting Information). They all showed much lower sensitivity and higher determination limit compared with those of the ultrasmall MoS_2 nanoparticle modified electrode, and their amperometric responses decreased with the increase of the sizes of the MoS_2 particles at the same level of the H_2O_2 concentration. Furthermore, they no longer exhibited high sensitivity toward H_2O_2 concentration at nanomolar levels. Even for the electrode modified with MoS_2 particles of tens of nanometers in size obtained by gradient centrifugation, such low sensitivity could not be achieved (Figure S15 in the Supporting Information). This is in accordance with the fact that numerous experimental investigations of nanostructured metal-oxide films revealed a strong increase in sensitivity when the average grain size was reduced to several nanometers.[59,60]

The similar size dependence was observed for the electro-catalysis of HER and ORR at different sizes of MoS_2 particles modified electrodes in our previous work.[48] These further confirm that the excellent electrocatalytic performance of the ultrasmall MoS_2 nanoparticle modified electrode toward reduction of H_2O_2 originates from the size effect. The smaller the sizes of MoS_2 particles are, the more the surface active sites are and the better the electrocatalytical activity is. The real determination limit was 2.5 nM (Figure 6), which was much
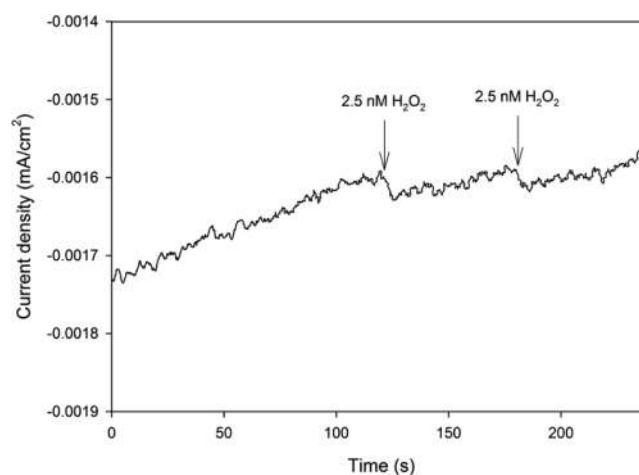

Figure 6. Determination limit of the ultrasmall MoS_2 nanoparticles modified electrode.

lower than that of most of the reported H_2O_2 sensors.[29,30,42] The reproducibility of the modified electrode was also tested. The relative standard derivation (RSD) of its current response for the addition of 2.00 μM H_2O_2 was 5.5% for 8 successive measurements, which suggested good precision. The anti-interference effect of the sensor toward ascorbic acid (AA) and uric acid (UA) was also investigated. AA and UA are two of the most commonly existing interference species in the physio-logical environment. Figure S16 in the Supporting Information showed the current responses of the sensor with the addition of 0.0500 mM H_2O_2, 0.100 mM AA, and 0.500 mM UA, respectively. The response current of the sensor changed greatly after the addition of H_2O_2, while nearly no current change could be observed with the addition of high concentrations of AA or UA. This verified that the sensor had good selectivity.

The constructed sensor was then used for the real-time tracking of H_2O_2 released by Raw 264.7 cells due to its low determination limit, good reproducibility, and selectivity. *N*-Formylmethionyl-leucyl-phenylalanine (fMLP) was used to stimulate the cells to generate H_2O_2. Around 2×10^6 cells were resuspended in 20 mL of PBS (pH = 7.4) for electrochemical measurement. After treated with 0.3 μM fMLP, an obvious current change that corresponding to 20 nM H_2O_2 could be observed, while no signal could be observed if cells were not treated with fMLP (Figure 7). This result was similar to the
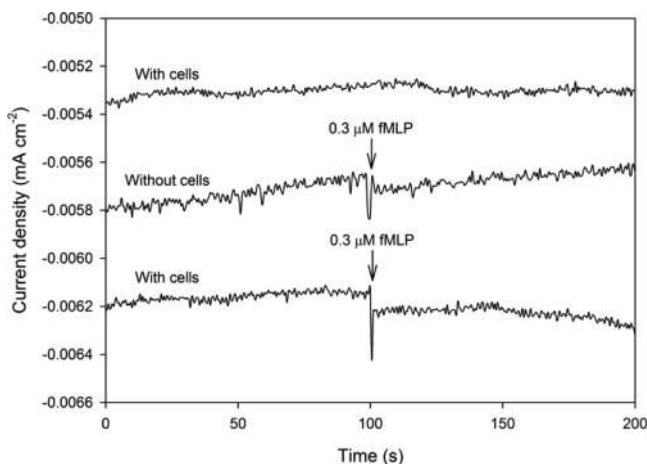

Figure 7. Amperometric responses of the ultrasmall MoS_2 nanoparticles modified electrode to the addition of 0.3 μM fMLP with and without Raw 264.7 cells as well as in the presence of Raw 264.7 cells without fMLP in the N_2 saturated 0.1 M PBS at −0.25 V.

result reported by Sun and his co-workers,[32] but they employed precious metals Pt and Pd. The response current of the sensor would only change slightly with the stimulation of 0.3 μM fMLP without the cells. If catalase was mixed with the PBS that contained cells, the intensity of the current response of the sensor would decrease greatly with the addition of fMLP (Figure S17 in the Supporting Information). And its intensity was similar to that obtained from the solution without cells (about $4-5 \times 10^{-5}$ mA cm^{-2}). This phenomenon proves that the obvious current change in Figure 7 in the presence of cells (about 1×10^{-4} mA cm^{-2}) originates from H_2O_2 produced from the cells, because catalase is a selective catalyst for the decomposition of H_2O_2. The recoveries of this biosensor were tested to be ∼85%−114% by spiking 20−50 nM H_2O_2 into the cell samples; moreover, the repeated measurements in Figure S18 in the Supporting Information gave similar current responses, which indicated that the sensor was credible.

A glucose biosensor was further developed based on the ultrasmall MoS_2 nanoparticles modified electrode since it exhibited highly catalytic activity toward the reduction of H_2O_2. Glucose oxidase (GOD) was immobilized on the MoS_2 nanoparticles films, and its CV responses in O_2 saturated 0.1 M PBS containing different concentrations of glucose were recorded (Figure 8). The reduction current of this glucose sensor increased with the increase of glucose concentration. Both O_2 and H_2O_2 would contribute to the reduction current of the glucose sensor. Even though the oxidization of glucose would consume O_2, the overall current response would still increase since the produced H_2O_2 would lead to more obvious current change. The current response of the glucose biosensor at −0.7 V was chosen for the linear fitting of the calibration
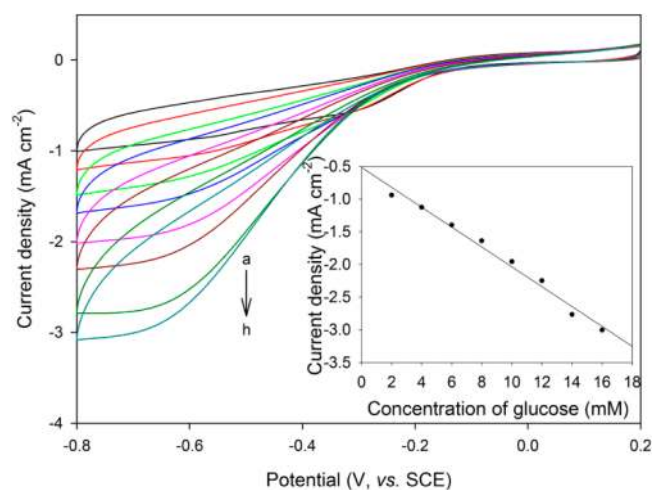

Figure 8. CV of the MoS_2/GOD modified electrode in the O_2 saturated 0.1 M PBS containing various concentrations of glucose: (a) 2.00, (b) 4.00, (c) 6.00, (d) 8.00, (e) 10.0, (f) 12.0, (g) 14.0, and (h) 16.0 mM from up to down at a scan rate of 50 mV s^{-1}. The inset is the calibration curve of the current response to the concentration of glucose from 2.00 mM to 16.0 mM at −0.7 V.

curve. A linear relationship between the peak current and the glucose concentration ranging from 2.00 mM to 16.0 mM was obtained for this sensor, which made it suitable for the determination of the normal blood sugar concentration (4−6 mM) in humans. The sensitivity of the glucose biosensor was 152 mA cm^{-2} M^{-1} and the RSD of its current response to 6.00 mM glucose was 1.9% for 7 replicate measurements. The sensor also had good stability. After storage in a refrigerator for 2 weeks, it remained 93.6% of its initial current response. This glucose biosensor was then used to detect the blood sugar concentration of a health person and the result was 5.77 mM (Figure S19 in the Supporting Information), which is in accordance with the result of 5.45 mM obtained from a hospital. The recoveries of the glucose biosensor were also investigated by spiking 2.00−4.00 mM glucose into the blood samples, and the results ranged from 91.0% to 108%. All of these revealed that the sensor was applicable to the detection of the blood glucose in humans.

■ CONCLUSION

In conclusion, by controlling the MoS_2 particle size, we engineered the surface structure at the atomic scale and preferentially exposed more catalytically active edge sites, enabling improved electrocatalytic performance toward H_2O_2 reduction. We have fabricated a H_2O_2 biosensor based on ultrasmall MoS_2 nanoparticles with high sensitivity and selectivity by a simple way without any enzymes. Its determination limit was as low as 2.5 nM and could be used for the detection of the trace amount of H_2O_2 released by the cells. More importantly, the high activity of the MoS_2 nanoparticle modified electrode toward the reduction of H_2O_2 made it a platform for the construction of some other biosensors like the glucose sensor because H_2O_2 is a product of many oxidative biological reactions. This MoS_2 nanoparticles based sensor can be easily constructed on a flexible substrate, which would enable its miniaturization, and enable its integration in lab-on-chip devices or in intracellular H_2O_2 detection. Research efforts along these directions are expected to have potential commercial application since the preparation

method of ultrasmall MoS$_2$ nanoparticles is very simple and convenient.

ASSOCIATED CONTENT

Supporting Information

Some supplemental figures. This material is available free of charge via the Internet at http://pubs.acs.org.

AUTHOR INFORMATION

Corresponding Authors
*E-mail: linjian@pku.edu.cn.
*E-mail: lmwx@pku.edu.cn.

Notes
The authors declare no competing financial interest.

ACKNOWLEDGMENTS

REFERENCES

(1) Nossol, E.; Zarbin, A. J. G. Adv. Funct. Mater. 2009, 19, 3980−3986.

(2) DeYulia, G. J.; Cárcamo, J. M.; Bórquez-Ojeda, O.; Shelton, C. C.; Golde, D. W. Proc. Natl. Acad. Sci. U.S.A. 2005, 102, 5044−5049.

(3) Winterbourn, C. C. Nat. Chem. Biol. 2008, 4, 278−286.

(4) Preston, T. J.; Muller, W. J.; Singh, G. J. Biol. Chem. 2001, 276, 9558−9564.

(5) Rhee, S. G. Science 2006, 312, 1882−1883.

(6) Abo, M.; Urano, Y.; Hanaoka, K.; Terai, T.; Komatsu, T.; Nagano, T. J. Am. Chem. Soc. 2011, 133, 10629−10637.

(7) Capasso, M.; Bhamrah, M. K.; Henley, T.; Boyd, R. S.; Langlais, C.; Cain, K.; Dinsdale, D.; Pulford, K.; Khan, M.; Musset, B.; Cherny, V. V.; Morgan, D.; Gascoyne, R. D.; Vigorito, E.; DeCoursey, T. E.; MacLennan, I. C. M.; Dyer, M. J. S. Nat. Immunol. 2010, 11, 265-U12.

(8) Belousov, V. V.; Fradkov, A. F.; Lukyanov, K. A.; Staroverov, D. B.; Shakhbazov, K. S.; Terskikh, A. V.; Lukyanov, S. Nat. Methods 2006, 3, 281−286.

(9) Matos, R. C.; Coelho, E. O.; de Souza, C. F.; Guedes, F. A.; Matos, M. A. Talanta 2006, 69, 1208−1214.

(10) Liu, Y. H. A.; Liao, X. B. Curr. Org. Chem. 2013, 17, 654−669.

(11) Srikun, D.; Albers, A. E.; Nam, C. I.; Iavaron, A. T.; Chang, C. J. J. Am. Chem. Soc. 2010, 132, 4455−4465.

(12) Shan, C. S.; Yang, H. F.; Han, D. X.; Zhang, Q. X.; Ivaska, A.; Niu, L. Biosens. Bioelectron. 2010, 25, 1070−1074.

(13) Guo, S. J.; Wen, D.; Zhai, Y. M.; Dong, S. J.; Wang, E. K. ACS Nano 2010, 4, 3959−3968.

(14) Hammond, P. T. Adv. Mater. 2004, 16, 1271−1293.

(15) Xiao, F.; Li, Y. Q.; Zan, X. L.; Liao, K.; Xu, R.; Duan, H. W. Adv. Funct. Mater. 2012, 22, 2487−2494.

(16) Qu, F. L.; Yang, M. H.; Shen, G. L.; Yu, R. Q. Biosens. Bioelectron. 2007, 22, 1749−1755.

(17) Liu, R. J.; Li, S. W.; Yu, X. L.; Zhang, G. J.; Zhang, S. J.; Yao, J. N.; Keita, B.; Nadjo, L.; Zhi, L. J. Small 2012, 8, 1398−1406.

(18) Ricci, F.; Palleschi, G. Biosens. Bioelectron. 2005, 21, 389−407.

(19) Li, J.; Qiu, J. D.; Xu, J. J.; Chen, H. Y.; Xia, X. H. Adv. Funct. Mater. 2007, 17, 1574−1580.

(20) Sun, N. J.; Guan, L. H.; Shi, Z. J.; Li, N. Q.; Gu, Z. N.; Zhu, Z. W.; Li, M. X.; Shao, Y. H. Anal. Chem. 2006, 78, 6050−6057.

(21) Xu, J.; Shang, F. J.; Luong, J. H. T.; Razeeb, K. M.; Glennon, J. D. Biosens. Bioelectron. 2010, 25, 1313−1318.

(22) Hrapovic, S.; Liu, Y. L.; Male, K. B.; Luong, J. H. T. Anal. Chem. 2004, 76, 1083−1088.

(23) Wen, Z. H.; Ci, S. Q.; Li, J. H. J. Phys. Chem. B 2009, 113, 13482−13487.

(24) Pingarrón, J. M.; Yáñez-Sedeño, P.; González-Cortés, A. Electrochim. Acta 2008, 53, 5848−5866.

(25) Zhou, M.; Zhai, Y. M.; Dong, S. J. Anal. Chem. 2009, 81, 5603−5613.

(26) Xu, X. A.; Jiang, S. J.; Hu, Z.; Liu, S. Q. ACS Nano 2010, 4, 4292−4298.

(27) Luo, Y. P.; Liu, H. Q.; Rui, Q.; Tian, Y. Anal. Chem. 2009, 81, 3035−3041.

(28) Lee, Y. M.; Garcia, M. A.; Huls, N. A. F.; Sun, S. H. Angew. Chem., Int. Ed. 2010, 49, 1271−1274.

(29) Liu, Y. X.; Dong, X. C.; Chen, P. Chem. Soc. Rev. 2012, 41, 2283−2307.

(30) Shao, Y. Y.; Wang, J.; Wu, H.; Liu, J.; Aksay, I. A.; Lin, Y. H. Electroanalysis 2010, 22, 1027−1036.

(31) Kim, G.; Lee, Y. E. K.; Xu, H.; Philbert, M. A.; Kopelman, R. Anal. Chem. 2010, 82, 2165−2169.

(32) Sun, X. L.; Guo, S. J.; Liu, Y.; Sun, S. H. Nano Lett. 2012, 12, 4859−4863.

(33) Lyon, J. L.; Stevenson, K. J. Anal. Chem. 2006, 78, 8518−8525.

(34) Karam, P.; Halaoui, L. I. Anal. Chem. 2008, 80, 5441−5448.

(35) Benavente, E.; Santa Ana, M. A.; Mendizábal, F.; González, G. Coord. Chem. Rev. 2002, 224, 87−109.

(36) Hinnemann, B.; Moses, P. G.; Bonde, J.; Jørgensen, K. P.; Nielsen, J. H.; Horch, S.; Chorkendorff, I.; Nørskov, J. K. J. Am. Chem. Soc. 2005, 127, 5308−5309.

(37) Jaramillo, T. F.; Jørgensen, K. P.; Bonde, J.; Nielsen, J. H.; Horch, S.; Chorkendorff, I. Science 2007, 317, 100−102.

(38) Li, Y. G.; Wang, H. L.; Xie, L. M.; Liang, Y. Y.; Hong, G. S.; Dai, H. J. J. Am. Chem. Soc. 2011, 133, 7296−7299.

(39) Merki, D.; Fierro, S.; Vrubel, H.; Hu, X. L. Chem. Sci. 2011, 2, 1262−1267.

(40) Radisavljevic, B.; Radenovic, A.; Brivio, J.; Giacometti, V.; Kis, A. Nat. Nanotechnol. 2011, 6, 147−150.

(41) Feng, J.; Qian, X. F.; Huang, C. W.; Li, J. Nat. Photon. 2012, 6, 865−871.

(42) Chen, D.; Feng, H. B.; Li, J. H. Chem. Rev. 2012, 112, 6027−6053.

(43) Xiao, F.; Song, J. B.; Gao, H. C.; Zan, X. L.; Xu, R.; Duan, H. W. ACS Nano 2012, 6, 100−110.

(44) Zeng, Q. O.; Cheng, J. S.; Tang, L. H.; Liu, X. F.; Liu, Y. Z.; Li, J. H.; Jiang, J. H. Adv. Funct. Mater. 2010, 20, 3366−3372.

(45) Wu, S. X.; Zeng, Z. Y.; He, Q. Y.; Wang, Z. J.; Wang, S. J.; Du, Y. P.; Yin, Z. Y.; Sun, X. P.; Chen, W.; Zhang, H. Small 2012, 8, 2264−2270.

(46) Jaouen, F.; Proietti, E.; Lefèvre, M.; Chenitz, R.; Dodelet, J. P.; Wu, G.; Chung, H. T.; Johnston, C. M.; Zelenay, P. Energy Environ. Sci. 2011, 4, 114−130.

(47) Laursen, A. B.; Kegnæs, S.; Dahl, S.; Chorkendorff, I. Energy Environ. Sci. 2012, 5, 5577−5591.

(48) Wang, T. Y.; Gao, D. L.; Zhuo, J. Q.; Zhu, Z. W.; Papakonstantinou, P.; Li, Y.; Li, M. X. Chem.—Eur. J. 2013, 19, 11939−11948.

(49) Lin, Y. H.; Lu, F.; Tu, Y.; Ren, Z. F. Nano Lett. 2004, 4, 191−195.

(50) Lu, J.; Do, I.; Drzal, L. T.; Worden, R. M.; Lee, I. ACS Nano 2008, 2, 1825−1832.

(51) Gill, R.; Bahshi, L.; Freeman, R.; Willner, I. Angew. Chem., Int. Ed. 2008, 47, 1676−1679.

(52) Pelossof, G.; Tel-Vered, R.; Elbaz, J.; Willner, I. Anal. Chem. 2010, 82, 4396−4402.

(53) Choucair, M.; Thordarson, P.; Stride, J. A. Nat. Nanotechnol. 2009, 4, 30−33.

(54) Hernandez, Y.; Nicolosi, V.; Lotya, M.; Blighe, F. M.; Sun, Z. Y.; De, S.; McGovern, I. T.; Holland, B.; Byrne, M.; Gun'ko, Y. K.; Boland, J. J.; Niraj, P.; Duesberg, G.; Krishnamurthy, S.; Goodhue, R.; Hutchison, J.; Scardaci, V.; Ferrari, A. C.; Coleman, J. N. Nat. Nanotechnol. 2008, 3, 563−568.

(55) Coleman, J. N.; Lotya, M.; O'Neill, A.; Bergin, S. D.; King, P. J.; Khan, U.; Young, K.; Gaucher, A.; De, S.; Smith, R. J.; Shvets, I. V.;

Arora, S. K.; Stanton, G.; Kim, H. Y.; Lee, K.; Kim, G. T.; Duesberg, G. S.; Hallam, T.; Boland, J. J.; Wang, J. J.; Donegan, J. F.; Grunlan, J. C.; Moriarty, G.; Shmeliov, A.; Nicholls, R. J.; Perkins, J. M.; Grieveson, E. M.; Theuwissen, K.; McComb, D. W.; Nellist, P. D.; Nicolosi, V. *Science* **2011**, *331*, 568−571.

(56) Wang, Q. H.; Kalantar-Zadeh, K.; Kis, A.; Coleman, J. N.; Strano, M. S. *Nat. Nanotechnol.* **2012**, *7*, 699−712.

(57) Wang, T. Y.; Liu, L.; Zhu, Z. W.; Papakonstantinou, P.; Hu, J. B.; Liu, H. Y.; Li, M. X. *Energy Environ. Sci.* **2013**, *6*, 625−633.

(58) Uehara, H.; Diring, S.; Furukawa, S.; Kalay, Z.; Tsotsalas, M.; Nakahama, M.; Hirai, K.; Kondo, M.; Sakata, O.; Kitagawa, S. *J. Am. Chem. Soc.* **2011**, *133*, 11932−11935.

(59) Michel, C. R.; Mena, E. L.; Martínez, A. H. *Talanta* **2007**, *74*, 235−240.

(60) Kennedy, M. K.; Kruis, F. E.; Fissan, H.; Mehta, B. R.; Stappert, S.; Dumpich, G. *J. Appl. Phys.* **2003**, *93*, 551−560.